# Evidence of Antiblockade in an Ultracold Rydberg Gas

Thomas Amthor,* Christian Giese,† Christoph S. Hofmann, and Matthias Weidemüller‡
*Physikalisches Institut, Universität Heidelberg, Philosophenweg 12, 69120 Heidelberg, Germany*
(Received 27 August 2009; published 8 January 2010)

We present the experimental observation of the antiblockade in an ultracold Rydberg gas recently proposed by Ates *et al.* [Phys. Rev. Lett. **98**, 023002 (2007)]. Our approach allows the control of the pair distribution in the gas and is based on a strong coupling of one transition in an atomic three-level system, while introducing specific detunings of the other transition. When the coupling energy matches the interaction energy of the Rydberg long-range interactions, the otherwise blocked excitation of close pairs becomes possible. A time-resolved spectroscopic measurement of the Penning ionization signal is used to identify slight variations in the Rydberg pair distribution of a random arrangement of atoms. A model based on a pair interaction Hamiltonian is presented which well reproduces our experimental observations and allows one to deduce the distribution of nearest-neighbor distances.

DOI: 10.1103/PhysRevLett.104.013001 PACS numbers: 32.80.Ee, 34.10.+x, 34.20.Cf, 67.85.−d

The long-range character of strong Rydberg-Rydberg interactions gives rise to a variety of phenomena. The interaction-induced suppression or blockade of excitation is one of the most striking effects. It has been demonstrated in a number of different realizations using ultracold gases of interacting Rydberg atoms [1–8]. One of the driving forces in the study of Rydberg blockade and spatial structure is the possible application for quantum information processing [9–11]. In certain configurations, the blockade can be overcome and atom pairs can selectively be excited at short distance. Specific geometric arrangements of three atoms have been identified which reduce a blocking due to dipole interactions [12].

A so-called antiblockade has recently been proposed for a three-level two-photon Rydberg excitation scheme where the van der Waals (vdW) interaction energy at a given atomic distance corresponds to the Autler-Townes splitting induced by the lower transition [13]. By exploiting the blockade and antiblockade in a controlled way, spatial correlations can be imposed on the excited atoms in an otherwise randomly arranged ultracold gas. Specific pair distances can thus be preferred or suppressed, which is of particular interest not only for quantum information, but also for a variety of applications of controlled interactions, such as resonant energy transfer [14–17], the creation of long-range molecules [18–20], or the study of quantum mechanical transport phenomena in chains [21,22]. Some recent experiments use small optical dipole traps to fix the distance between Rydberg atoms [7,8], but this technique does not allow one to prepare a large number of pairs at specific range of distances simultaneously.

In the characterization of the antiblockade [13], Ates *et al.* considered a lattice with fixed lattice constant, while tuning the interaction strength between the Rydberg atoms by changing the principal quantum number. An increased two-photon Rydberg excitation probability in a three-level scheme [see Fig. 1(a)] was predicted when interaction energy and Rabi frequency $\Omega_1$ of the lower transition match. In our experimental demonstration of this effect, a complementary approach is followed. Starting from an unstructured gas, we show that atomic pairs can be resonantly excited even at interatomic separations where the atomic interaction shift is much greater than the excitation linewidth. While keeping the quantum number fixed, the interaction strength is instead matched by picking specific atom pairs with appropriate interatomic distance. Our method of measuring this modification of the pair distribution by the antiblockade is based on the dynamics of atomic pairs under the influence of the forces exerted by the interactions, as explored in Ref. [23]. Given an attractive vdW interaction, the collision times of close pairs are shorter resulting in Penning ionization at shorter times. In this way we are able to identify even slight variations in the nearest-neighbor distance distribution. The problem of antiblockade in a randomly distributed gas is briefly discussed in [24], where a detection technique based upon counting statistics is proposed [3]. However, our collision method yields a more direct measure of the pair distances.

We describe the system in terms of an interacting two-atom system with the three atomic levels $|g\rangle$, $|e\rangle$, $|r\rangle$, corresponding to $5S$, $5P$, and Rydberg level of $^{87}$Rb, respectively [see Fig. 1(a)]. The calculations are based on the two-atom Hamiltonian $H = H_{\mathrm{at}} + H_{\mathrm{int}}$, where $H_{\mathrm{at}}$ represents the couplings within the three-level systems and $H_{\mathrm{int}} = V_{\mathrm{int}}(R)|rr\rangle\langle rr|$ is the vdW interaction between two Rydberg states with $V_{\mathrm{int}}(R) = -C_6^{\mathrm{eff}}/R^6$. The interaction of atoms with nonvanishing angular momentum leads to a large number of interaction potentials due to the many possible symmetries. We introduce an effective vdW coefficient $C_6^{\mathrm{eff}}$ to reduce the calculation to a three-level system [23]. We solve the master equation for the density matrix, $\dot{\sigma} = -\frac{i}{\hbar}[H, \sigma] + \Gamma$, where $\Gamma$ contains the decay of the intermediate state $\gamma = 2\pi \times 6$ MHz as well as the laser linewidths ($\sim 2\pi \times 1$ MHz) as additional dephasing

 

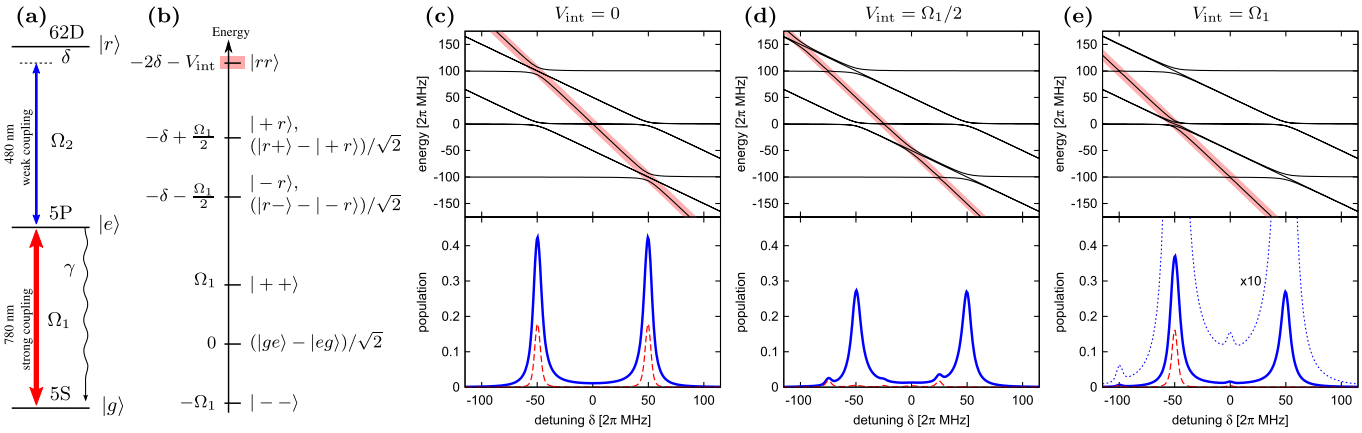


FIG. 1 (color online). (a) Atomic level scheme. The states $5S$ and $5P$ of $^{87}$Rb are coupled by a strong resonant laser field, while the weak upper laser coupling is detuned from the Rydberg state 62D by $\delta$. (b) Dressed pair state energies for $|\delta| \gg \Omega_1$ with $|\pm\rangle = (|e\rangle \pm |g\rangle)/\sqrt{2}$. (c)–(d) Eigenstates (upper graphs) and calculated Rydberg excitation (lower graphs) as a function of $\delta$ for fixed pair distance corresponding to $V_{\rm int} = 0$, $V_{\rm int} = \Omega_1/2$, $V_{\rm int} = \Omega_1$, respectively. The Rabi frequencies are $\Omega_1 = 2\pi \times 100$ MHz and $\Omega_2 = 2\pi \times 10$ MHz. For $|\delta| \gg \Omega_1$ the states approach the ones shown in (b). The states containing predominantly $|rr\rangle$ character are highlighted with a thick (red) line. In the excitation spectra, the solid blue lines represent the total Rydberg population per atom, while the dashed red lines show the population of the Rydberg pair state $|rr\rangle$. The dotted line in (e) is the total population scaled by a factor of 10. Parameters and excitation laser pulse shape correspond to the experimental settings.

terms. The spontaneous and blackbody induced decay of the Rydberg level can be neglected here because the time scale of observation is well below the time scale of these processes for the Rydberg state chosen in the experiment [25].

We introduce the detuning from the Rydberg state $\delta$ and the Rabi frequencies $\Omega_1$ and $\Omega_2$ for the two transitions with $\Omega_1 \gg \Omega_2$, $\gamma$. The dressed eigenenergies of two interacting three-level systems are given explicitly in Fig. 1(b) for the limiting case of $|\delta| \gg \Omega_1$, and are plotted in Figs. 1(c)–1(e) (upper graphs) as a function the detuning. Lines with slope $-1$ correspond to levels containing one Rydberg excitation, while lines with slope $-2$ (highlighted with a thick red line) contain predominantly $|rr\rangle$ character. At the avoided crossings the Rydberg states are populated, resulting in the well-known Autler-Townes doublet.

Calculated Rydberg excitation spectra for pairs at three different separations, i.e., for three different interaction energies $V_{\rm int}$, are depicted in Figs. 1(c)–1(e) (lower graphs). Without interaction (atoms far apart), a symmetric Autler-Townes spectrum is visible [Fig. 1(c)] and the population of $|rr\rangle$ (red dotted line) is equal on both peaks. An interaction energy of $V_{\rm int} = \Omega_1/2$ [Fig. 1(d)] causes a considerable blockade of excitation, with the population of the state $|rr\rangle$ being completely suppressed at the two resonances, but slightly enhanced on the side of each excitation line corresponding to lower laser frequencies. In the corresponding energy diagram, the state containing predominantly $|rr\rangle$ character is shifted. If $V_{\rm int}$ is further increased to match the lower Rabi frequency $\Omega_1$ [Fig. 1(e)], the doubly excited state $|rr\rangle$ is again populated at $\delta = -\Omega_1/2$, but is still completely suppressed at $\delta = +\Omega_1/2$. As can be seen in the energy diagram, the state experiencing the interaction shift now crosses zero at $\delta = -\Omega_1/2$, while there is no possible coupling any more for $\delta > 0$. A slight enhancement of excitation can also be observed at $\delta = 0$ (see dotted curve). The antiblockade discussion in [13] is restricted to this peak at zero detuning. Introducing a finite detuning of $\delta = -\Omega_1/2$, the antiblockade effect becomes much more pronounced. In addition, it is now possible to directly compare a blocked regime (positive detuning) with an antiblocked regime (negative detuning) in a single spectrum.

In order to predict the outcome of a measurement in an unstructured cloud, one determines weighted averages of spectra at different interatomic spacings representing the actual distribution of nearest-neighbor distances [26]. The results of such a calculation for our experimental parameters are presented in Fig. 2(a). The same scaling factor is used for all graphs to match the experimental detector signal of the Rydberg excitation. The upper graph (black) represents the total Rydberg excitation with contributions of $|gr\rangle$, $|rg\rangle$, $|er\rangle$, $|re\rangle$, and $|rr\rangle$, averaged over all nearest-neighbor distances. The lower graphs (red) show only the population of $|rr\rangle$ as an average of all pair distances at which the atoms are undergoing Penning ionization within the specified time delay. This implicitly assumes that each collision leads to Penning ionization with unity probability. As expected from Fig. 1, one finds a pronounced asymmetry of the two Autler-Townes components. Because of the attractive character of the interaction potential, ions appear first on the side of each of the $62D_{5/2}$ lines corresponding to lower laser frequencies [23]. The collision time depends mainly on the long-range part of the attractive interaction potentials, where the atom pairs spend most of their time. This is why one does not require exact knowledge of the inner part of the potentials.

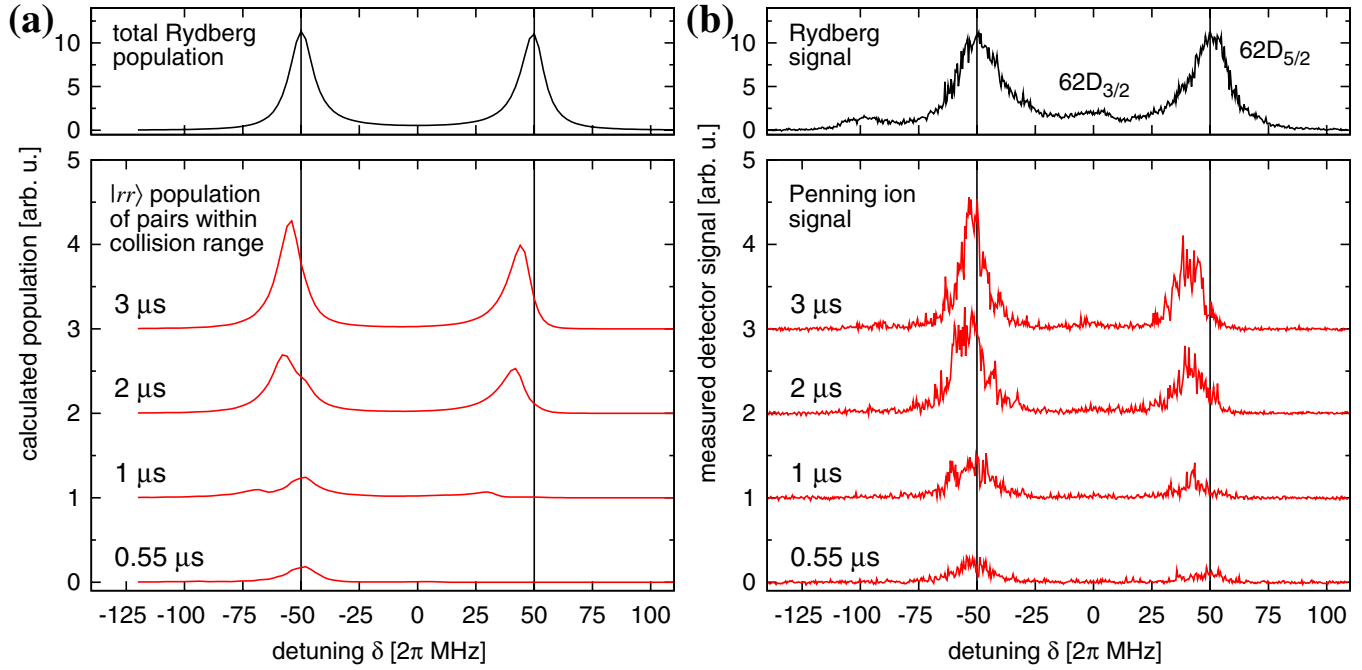


FIG. 2 (color online). Comparison between (a) calculated and (b) measured 62D Rydberg excitation and ionization spectra for $\Omega_1 = 2\pi \times 100$ MHz, $C_6^{\text{eff}} = 5 \times 10^{20}$ a.u., and a density of the trapped ground state atoms of $7 \times 10^9$ cm$^{-3}$. The upper graphs in each set (black) show the Rydberg population directly after excitation. Below (red) the ion signal at different delay times is shown, offset vertically for clarity. The respective delay $\Delta t$ is indicated at each trace. In both model and measurement, ions appear earlier on the red-detuned Autler-Townes component. A redshift of the maximum ionization relative to each peak in the excitation spectrum is always clearly visible. Vertical lines are drawn at $\pm 50$ MHz to emphasize this.

In the experiment, atoms confined in a magneto-optical trap are excited to the $62D$ state with a 50 ns pulse of the upper transition, while the lower transition laser is turned on with a fixed Rabi frequency $\Omega_1$. The lower (red) laser illuminates the whole trapped atom cloud, and the upper (blue) laser is focused to a waist of 37 $\mu$m, resulting in a peak Rabi frequency of $\Omega_2^{\text{peak}} = 2\pi \times 10.6$ MHz in the center. After a delay time $\Delta t$, an electric field ramp is applied to drive the ions onto a microchannel plate detector. Ions already present due to Penning ionization are detected first, while the remaining Rydberg atoms are only ionized when the field is strong enough and can thus be distinguished in the detector signal. The experimental cycle is repeated every 70 ms. Each cycle yields one data point in the measured Rydberg and ionization spectra presented in Fig. 2(b). The structure of the $62D_{3/2}$ and $62D_{5/2}$ lines appears twice in the spectrum, separated by the lower Rabi frequency. We restrict our discussion to $62D_{5/2}$, as $62D_{3/2}$ is only weakly excited. Excellent agreement between our model and the measurements is found for an effective attractive vdW interaction with $C_6^{\text{eff}} = 5 \times 10^{20}$ a.u. This value is consistent with long-range potential calculations [27] for the state $62D_{5/2}$ which yield values of the same order of magnitude for all possible molecular symmetries. In accordance with theory, there is a clear asymmetry between the two Autler-Townes components. The ionization is stronger and starts earlier on the component which appears at $\delta < 0$, as expected from the above reasoning. Clearly, the excitation of close pair states is suppressed for the peak at positive detuning (blockade), while it is allowed for the peak at negative detuning (anti-blockade). The contribution of these Rydberg pairs $|rr\rangle$ at short distances, which are subject to early Penning ionization, is hardly discernible in the total Rydberg signal (upper graph).

The distinctness of the asymmetry depends on the availability of atom pairs for which the interaction potential corresponds to $\Omega_1$. As the ground state pair density for a separation $R$ is proportional to $R^2$, more pairs are available at larger distances, which is why the asymmetry becomes more pronounced for smaller Rabi splittings $\Omega_1$. We have verified this with additional measurements and calculations at $V_{\text{int}} = 2\pi \times 62$ MHz and $V_{\text{int}} = 2\pi \times 150$ MHz. In all calculations and measurements, the asymmetry of the two peak heights also consistently decreases as the ion peaks grow with time. At these large Rabi splittings $\Omega_1$ we specifically access and probe variations of the pair distances below the average distance of atoms in the cloud. This allows us to describe the system in terms of nearest neighbors and to neglect many-body effects.

The underestimation of the peak widths in the simulation can be explained by the fact that we did not consider the spatial intensity profile of the upper excitation laser but instead only used the Rabi frequency present in the center of the beam to minimize calculation time. Averaging over the radial distribution of Rabi frequencies induced by the

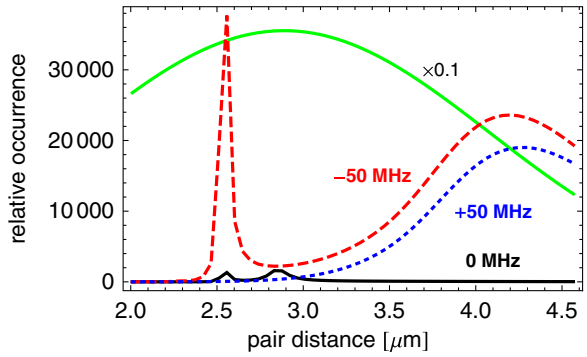


FIG. 3 (color online). Calculated nearest-neighbor pair distribution of $|rr\rangle$ states for $\Omega_1 = 2\pi \times 100$ MHz and $\delta = 0$ (black, solid), $\delta = 2\pi \times 50$ MHz (blue, dotted), and $\delta = -2\pi \times 50$ MHz (red, dashed), at $\Delta t = 0$. The solid green curve above shows the ground state nearest-neighbor distribution, scaled by a factor of 0.1 for better visibility.

upper excitation laser has been found to account for a slight broadening of the excitation peaks [28]. We observe that a small number of ions appear already at very short times (0.55 $\mu$s), before the first collisions are predicted by our model. This might be attributed to a resonant coupling as discussed in Ref. [29].

The difference in the distribution of pair distances at the position of the two Autler-Townes peaks $\delta = \pm\Omega_1/2$ is plotted in Fig. 3. The green solid line represents the distribution of nearest-neighbor distances in the cloud. At $\delta = +\Omega_1/2$ (blue dotted line) the population of $|rr\rangle$ is strongly suppressed at distances below 3.5 $\mu$m. At $\delta = -\Omega_1/2$ (red dashed line) additional pairs at small distances ($\sim$2.5 $\mu$m) are present where the pair distance leads to an interaction energy $V_{\text{int}}$ close to $\Omega_1$. At zero detuning (solid black line) there is also a finite excitation probability at small distances, but the excitation is still comparatively small because of the strong Autler-Townes splitting.

In conclusion, we have observed and modeled the effects of an antiblockade in an interacting Rydberg gas excited with a strong coupling laser at the lower transition of a three-level system. We used time-resolved ionization detection as a method to monitor the distribution of excited pair distances which allowed us to clearly observe additionally excited pairs at small distances out of a large distribution. The model calculation based on interacting atom pairs shows excellent agreement with the measured ionization dynamics. Making use of detuned excitation, we are able to directly manipulate the Rydberg pair distribution through long-range interactions and to compare a blocked and an antiblocked situation in a single spectrum. The asymmetry between the two ionization peaks is a direct probe for the strength of Rydberg interactions. Since our method does not require us to arrange the atoms but rather creates structure within an initially unordered gas, it may be used in experiments requiring large numbers of atom pairs, e.g., as an initialization or detection step in quantum gate experiments. In future experiments it may become possible to observe the antiblockade effect in its most drastic manifestation, when the atoms are arranged in a lattice with fixed interatomic distances.

The authors acknowledge financial support by the Deutsche Forschungsgemeinschaft (Grant No. WE2661/10-1). We thank C. Ates, T. Pohl, and J.-M. Rost for stimulating discussions.

*amthor@physi.uni-heidelberg.de
†Permanent address: Universität Freiburg, Hermann-Herder-Straße 3, 79104 Freiburg, Germany.
‡weidemueller@physi.uni-heidelberg.de

[1] D. Tong *et al.*, Phys. Rev. Lett. **93**, 063001 (2004).
[2] K. Singer *et al.*, Phys. Rev. Lett. **93**, 163001 (2004).
[3] T. Cubel Liebisch, A. Reinhard, P. R. Berman, and G. Raithel, Phys. Rev. Lett. **95**, 253002 (2005).
[4] T. Vogt *et al.*, Phys. Rev. Lett. **97**, 083003 (2006).
[5] T. Vogt *et al.*, Phys. Rev. Lett. **99**, 073002 (2007).
[6] R. Heidemann *et al.*, Phys. Rev. Lett. **99**, 163601 (2007).
[7] E. Urban *et al.*, Nature Phys. **5**, 110 (2009).
[8] A. Gaëtan *et al.*, Nature Phys. **5**, 115 (2009).
[9] D. Jaksch *et al.*, Phys. Rev. Lett. **85**, 2208 (2000).
[10] M. D. Lukin *et al.*, Phys. Rev. Lett. **87**, 037901 (2001).
[11] E. Brion, L. H. Pedersen, and K. Mølmer, J. Phys. B **40**, S159 (2007).
[12] T. Pohl and P. R. Berman, Phys. Rev. Lett. **102**, 013004 (2009).
[13] C. Ates, T. Pohl, T. Pattard, and J. M. Rost, Phys. Rev. Lett. **98**, 023002 (2007).
[14] W. R. Anderson, J. R. Veale, and T. F. Gallagher, Phys. Rev. Lett. **80**, 249 (1998).
[15] I. Mourachko *et al.*, Phys. Rev. Lett. **80**, 253 (1998).
[16] S. Westermann *et al.*, Eur. Phys. J. D **40**, 37 (2006).
[17] C. S. E. van Ditzhuijzen *et al.*, Phys. Rev. Lett. **100**, 243201 (2008).
[18] C. H. Greene, A. S. Dickinson, and H. R. Sadeghpour, Phys. Rev. Lett. **85**, 2458 (2000).
[19] C. Boisseau, I. Simbotin, and R. Côté, Phys. Rev. Lett. **88**, 133004 (2002).
[20] V. Bendkowsky *et al.*, Nature (London) **458**, 1005 (2009).
[21] R. Côté, A. Russell, E. E. Eyler, and P. L. Gould, New J. Phys. **8**, 156 (2006).
[22] O. Mülken *et al.*, Phys. Rev. Lett. **99**, 090601 (2007).
[23] T. Amthor *et al.*, Phys. Rev. Lett. **98**, 023004 (2007).
[24] C. Ates, T. Pohl, T. Pattard, and J. M. Rost, Phys. Rev. A **76**, 013413 (2007).
[25] I. I. Beterov *et al.*, New J. Phys. **11**, 013052 (2009).
[26] P. Hertz, Math. Ann. **67**, 387 (1909).
[27] K. Singer, J. Stanojevic, M. Weidemüller, and R. Côté, J. Phys. B **38**, S295 (2005).
[28] J. Deiglmayr *et al.*, Opt. Commun. **264**, 293 (2006).
[29] P. J. Tanner, J. Han, E. S. Shuman, and T. F. Gallagher, Phys. Rev. Lett. **100**, 043002 (2008).